Published in final edited form as:
Exp Cell Res. 2012 October 1; 318(16): 2143–2152. doi:10.1016/j.yexcr.2012.06.005.

Tissue protection and endothelial cell signaling by 20-HETE analogs in intact *ex vivo* lung slices

Elizabeth R. Jacobs[1,2,4], **Sreedhar Bodiga**[1,2], **Irshad Ali**[1,2], **Aaron M. Falck**[5], **John R. Falck**[5], **Meetha Medhora**[1,2,3], and **Anuradha Dhanasekaran**[1,2]

[1]Department of Medicine, Medical College of Wisconsin, Milwaukee, WI 53226

[2]Cardiovascular Center, Medical College of Wisconsin, Milwaukee, WI 53226

[3]Department of Radiation Oncology, Medical College of Wisconsin, Milwaukee, WI 53226

[4]Clement J. Zablocki VA Medical Center, 5000 W. National Ave, Milwaukee WI 53294

[5]Department of Biochemistry, University of Texas Southwestern Medical Center, Dallas, Tx 75390

Abstract

The capacity to follow cell type-specific signaling *in intact lung* remains limited. 20-hydroxyeicosatetraenoic acid (20-HETE) is an endogenous fatty acid that mediates signaling for a number of key physiologic endpoints in the pulmonary vasculature, including cell survival and altered vascular tone. We used confocal microscopy to identify enhanced reactive oxygen species (ROS) production in endothelial cell (EC)s in intact lung evoked by two stable analogs of 20-HETE, 20-5,14-HEDE (20-hydroxyeicosa-5(Z),14(Z)-dienoic acid) and 20-5,14-HEDGE (N-[20-hydroxyeicosa-5(Z),14(Z)-dienoyl]glycine). These analogs generated increased ROS in cultured pulmonary artery endothelial cells as well. 20-HETE analog treatment decreased apoptosis of pulmonary tissue exposed to hypoxia-reoxygenation (HR) *ex vivo*. Enhanced ROS production and apoptosis were confirmed by biochemical assays. Our studies identify physiologically critical, graded ROS from ECs in live lung tissue *ex vivo* treated with 20-HETE analogs and protection from HR-induced apoptosis. These methodologies create exciting possibilities for studying signaling by stable 20-HETE analogs and other factors in pulmonary endothelial and other lung cell types in their native milieu.

Keywords

dihydroethidium; eicosanoid; reactive oxygen species; TUNEL; confocal

Introduction

Reactive oxygen species (ROS) have been implicated as mediators of cellular proliferation/survival as well as cell death, depending on the amount, source and trigger. In pulmonary artery endothelial cells, one trigger for increased ROS *and* enhanced survival is treatment with the cytochrome P450 metabolite 20-hydroxyeicosatetraenoic acid (20-HETE) or

Corresponding author: Elizabeth R. Jacobs, MD MBA, Clement J. Zablocki VA Medical Center, 5000 W. National Ave, Milwaukee WI 53294, Tele: 414 384 2000 X41430, FAX: 414 382 5374, Elizabeth.Jacobs@va.gov.

analogs of the same. Although 20-HETE has pro-apoptotic actions in some organ systems [1,2], we have extensive evidence demonstrating anti-apoptotic action in lung tissue [3,4,5]. In cultured pulmonary artery endothelial cells (ECs), the pro-survival effects of this lipid are attributable to modest increments in superoxide production which appears to derive in part from NADPH oxidase and ROS [4,5]. However, studies with isolated cells provide little information about the physiological interactions that occur *in situ* when endothelial and other lung cells are juxtaposed. Therefore we developed a novel model to examine the effect of 20-HETE analogs on superoxide production from pulmonary artery and capillary ECs with intact physico-chemical interactions to other cell types. We describe a method for preparation of rodent lung slices to detect endothelial-specific effects of ROS production using dihydroethidium (DHE) fluorescence and CD31 (platelet endothelial cell adhesion molecule-1, or PECAM) staining. Previous models described by others [6,7] did not permit cell-type specific quantification of ROS production. We extended our model to study protection by 20-HETE analogs from apoptosis induced by *ex-vivo* hypoxia-reoxygenation in intact lung slices. This approach opens new avenues for unraveling the functional significance of 20-HETE analog-stimulated pulmonary endothelium-derived ROS in lung disease, and allows for direct visualization of local signaling events within the endothelial microenvironment.

Materials and Methods

20-HETE (hydroxyeicosatetraenoic acid), 20-5,14-HEDE (20-hydroxyeicosa-5(Z),14(Z)-dienoic acid) and 20-5,14-HEDGE (N-[20-hydroxyeicosa-5(Z),14(Z)-dienoyl]glycine) were synthesized in the laboratories of Dr. John Falck. Figure 1 shows the structures of these compounds. The 20-HETE analogs have advantages over native 20-HETE in that they are not subject to autoxidation. Varying degrees of autoxidation increase variability in experimental endpoints of interest. In addition, the analogs are not substrates for cyclooxygenase or lipoxygenase. Non-enzymatic oxidation products of arachidonic acid and polyunsaturated fatty acids such as isoprostanes have important effects on lung biology [8], as do cyclooxygenase products of 20-HETE [9]. Both analogs had qualitatively similar effects on DHE fluorescence in cultured PAECs and lung slices (see figure 2) as well as endpoints of interest in our published studies of 20-HETE in the lung [4,5,10]. For each set of experiments, one or the other analog was used as identified in the text and graphs.

Isolation and preparation of pulmonary artery endothelial cells (PAECs)

Bovine PAECs were isolated in a manner previously described by us [3]. Cells were grown to 80% confluence and made quiescent by removal of serum for six hours. Cells were used between passages 2 and 5, and loaded with a final concentration of 10 μM DHE for 10 minutes before washing. They were stimulated with vehicle, 20-HETE or analogs in final concentrations of 1 μM. BSA (0.1%) was added as a lipid carrier before fluorescence imaging.

Preparation and staining of lung slices with DHE and PECAM

Animal protocols were approved by the Institutional Animal Care and Use Committee at the Medical College of Wisconsin. Lungs were harvested from adult female rats Wistar (WAG/Rij/Cmcr) under deep anesthesia and rinsed in phosphate buffered saline (PBS). Unfrozen, intact lung tissue (~5×5×5 mm) was held in place by 2% agarose blocks, then 300 μm sections were obtained on a transverse plane with a microtome (OTS-4000, Electron Microscopy Sciences, Hatfield, PA). Lung sections were collected in iced PBS, then transferred to Dulbecco's modified essential media (DMEM), where they were incubated with polyethylene glycol coupled superoxide dismutase (PEG-SOD; cat #S9549 Sigma) or vehicle, then 10 μM dihydroethidium (DHE) for 10 min at 37μC. After washing and

transferring to fresh DMEM, lung slices were treated with vehicle (ethanol) or 20-HETE analog (1 μM) for 15 minutes. After a final rinse in PBS, lungs were imaged straight away or fixed for 90 minutes with 4% paraformaldehyde and PBS. Fixed sections were treated with primary antibody for CD31 (cat# 550300, BD Pharmingen) and examined in a confocal microscope. To confirm specificity of the stain, some thick sections were frozen in OCT compound and 10 micron sections prepared for imaging as below.

Fluorescence imaging

For some experiments as indicated in the text, a Nikon Eclipse TE2000-U with a camera attachment (Qimaging QCAM FAST394) was used to acquire fluorescent images. For confocal microscopic data acquisition, an inverted microscope (Zeiss Axiovert 510, Carl Zeiss), equipped with a three-line (488, 569, and 647 nm) argon-krypton laser, was used for excitation of the DHE and fluorescein isothiocyanate (FITC) labels. For DHE, a 610–650-nm band pass filter was employed with excitation at 488 nm using an argon laser; for FITC, a 505–550 nm band pass emission filter was used, with excitation at 488 nm using an argon laser from each tissue slice. Rhodamine-tagged terminal deoxynucleotidyl transferase mediated dUTP Nick End Labeling (TUNEL) positive cells were identified by excitation at 555 nm and detection at 580 nm. To avoid cross-talk between the fluorescence channels, probes were scanned sequentially.

Imaging experiments were performed at room temperature. Detector and laser settings were held constant across all samples within individual experiments, with control and experimental samples processed in each experiment. From each lung slice with confocal imaging, a Z stack containing 40–60 consecutive images was obtained.

Quantification of fluorescence

DHE fluorescence was quantified using Image J version 1.31, NIH analysis software by an investigator blinded to the treatment groups. The Red-Green-Blue confocal images were loaded into the program and converted to 8-bit gray-scale before subtracting background fluorescence equivalently for all images. From the stack of images, the slice with the peak intensity was identified; 2 confocal slices above and 2 below along with the slice with peak fluorescence were used for further image analysis. For some confocal experiments as indicated in the text, total fluorescence values for 5 slices were summated and expressed as a percentage of those for control (vehicle) samples. For endothelial cell-specific signals, a region of interest (ROI) was identified in overlaid red and green images of cells exhibiting green fluorescence from PECAM. The intensity of DHE signals in these cells was measured in the DHE channel. The total fluorescent output from all ROIs of 5 confocal images was summed and divided by the number of cells to determine the average DHE signal per EC. For cultured endothelial cells, the intensities of DHE fluorescence in ROIs placed over representative cells by an investigator blinded to the treatment group were summed and normalized to cell count to determine the DHE signal per cell.

Immunostaining of lung sections for smooth muscle actin, cytokeratin, PECAM-1, and DAPI

Lungs harvested from adult rats were embedded in Tissue-Tek OCT compound (Andwin Scientific, cat# 4583) and frozen sections (4 μM) were fixed in acetone or paraformaldehyde (as indicated in the text) for staining. We performed initial studies with primary antibodies for smooth muscle actin (Sigma-Aldrich, cat# A2547, 1:100; secondary Ab Invitrogen, Cat# A31571), cytokeratin (Cell Signaling Technology, cat# 4898, 1:100; secondary Ab Jackson ImmunoResearch Laboratories, Inc., cat# 711-166-152), and CD31 or PECAM (BD Pharmingen, cat# 550300, 1:50; secondary Alexa Fluor 488 Ab Invitrogen cat# A-11029) to identify the optimal conditions for cellular identification using these probes in our hands.

Non-immune serum was substituted for primary antibodies for negative staining controls. Slides were counterstained with a 4′,6′-diamino-2-phenylindole·2HCl (DAPI; Vector Laboratories, cat# H-1200) for nuclear identification.

Chemiluminescence assays

Lung pieces 10–30 mg in weight were treated with 20,5–14 HEDGE (1 μM) or vehicle (ethanol) in PBS for 15 minutes then transferred to a 96 well microplate well containing Henseleit-Krebs buffer. Lucigenin at a final concentration of 5 μM was added to each sample well through the injection port of a microplate reader (Modulus II Multimode Microplate Reader, Promega). Chemiluminescence was measured every 10 seconds over the next 5 minutes [11]. Data are expressed as change in relative luminescence units per unit time; relative light unit values normalized to gram wet lung weight per minute were also calculated.

Hypoxia-reoxygenation injury ex vivo

Lung slices treated with a single application of vehicle or 1 μM 20-HETE analog were maintained at 37 °C in humidified environments with 5% CO_2, balance air (normoxia) or 5% CO_2, balance nitrogen for 6 hours (hypoxia), followed by 1 hour in normoxia (reoxygenation; together HR). Apoptosis assays as below were performed on these tissues.

Apoptosis assays

After fixing, an Apoptag tag kit (Chemicon, cat # S7101) which marks nicked DNA terminals and a rhodamine tagged anti-digoxigenin Fab fragment (Roche Appl. Sci cat# 11207750910) was used to identify TUNEL positive ECs. To measure apoptosis biochemically, lung slices were processed as previously reported by us [4] for caspase-3 colorimetric activity assays (R&D Systems, cat. # BF3100).

Statistical analysis

Pooled data obtained in each experiment were used to calculate the means + standard errors for control (vehicle treated) or experimental (e.g. 20-HETE analog treated) samples. The data were tested for significance by a Student's *t*-test (for two samples) or Mann Whitney Rank Sum Test using the Jandel Corporation, SigmaStat Software. For experiments with more than 2 groups, ANOVA with post hoc Holm Sidak testing when permitted was performed. For chemiluminescence data, we assessed differences in vehicle- and 20-HETE-treated groups by measuring ANOVA on the rates of change per unit time. When permissible, post hoc pairwise Multiple Comparison Procedures by the Holm-Sidak method were completed. Experiments with $p<0.05$ were considered significant.

Results

20-5,14-HEDE and 20-5,14-HEDGE increase DHE fluorescence in cultured PAECs

One micromolar 20-HETE, 20-5,14-HEDE or 20-5,14-HEDGE increased DHE fluorescence over that of vehicle treated cells (figure 2a). Both analogs elicited greater increments in DHE than did 20-HETE alone, consistent with stimulated ROS production in these cells.

Measurement of increased superoxide in intact lung slices *ex vivo* after treatment with 20-5,14-HEDE or 20-5,14-HEDGE

Freshly cut lung slices (300 μm thick) loaded with DHE and imaged immediately after application of vehicle, 20-5,14-HEDE or 20-5,14-HEDGE exhibited DHE fluorescence as seen in representative images figure 2b and 2c. Both 20-5,14-HEDE and 20-5,14-HEDGE increased DHE fluorescence over that of vehicle (figures 2b and 2c). In data not shown, low

melting agarose-filled lungs produced a green autofluorescence which interfered with staining. Therefore this methodology was not further pursued.

To determine the component of the fluorescence signal with DHE attributable to superoxide, we treated lung slices with PEG-SOD (figure 2d). The majority of DHE fluorescence in vehicle treated slices remained after PEG-SOD, suggesting a non-specific or background nature to this portion of the signal. A substantial increase in fluorescence of 20-5,14-HEDGE–treated samples without PEG-SOD is observed. The difference between fluorescence intensity in analog-treated tissue with and without PEG-SOD is the component of the total fluorescence representing superoxide evoked by 20-5,14-HEDGE. These data are consistent with our previous reports of 20-HETE or analog-stimulated ROS production in isolated PAECs [3,5].

Colocalization of ROS in endothelial cells: Fixation and Labeling with PECAM-1 (CD31) antibody

Total DHE fluorescence was quantified in endothelial cells from lung slices treated with vehicle or 20-5,14-HEDE, then fixed with paraformaldehyde and secondarily immunostained with CD31 (PECAM-1, figure 3a). 20-5,14-HEDE increased DHE fluorescence over that of vehicle control quantitatively and qualitatively similar to that of unfixed slices (compare figures 3a and 3b to 2b). Next, CD31-associated DHE signal (figure 4a) was quantified as described in the methods. EC-associated ROS in 20-5,14-HEDE treated slices was increased over that of vehicle (figure 4b). We confirmed that treatment with 20-5,14-HEDE did not alter protein levels of PECAM-1 by western blot (data not shown).

Verification of PECAM-1 staining

To confirm specificity of immunostaining with anti-CD31 antibody in figure 4, frozen lung sections were conventionally prepared. Four micron sections of acetone fixed rat lung tissue were stained with different primary antibodies and imaged with the confocal microscope. These images demonstrate distinct patterns of staining consistent with smooth muscle cells in large and small pulmonary arteries (figure 5a), cytokeratin in epithelial cells (figure 5b) and PECAM (CD31) in endothelial cells (figure 5c). The anti-CD31 exhibited fluorescence in a lacy pattern staining capillary and vascular endothelial cells (figures 5c and 5d). This pattern was different in character than that for smooth muscle or keratin. We also obtained images from lung tissue fixed with paraformaldehyde (similar to the protocol used for thick slices) and immunostained with anti-CD31 antibody (figure 5d). A pattern of staining similar to that in figure 5c is observed. In all cases, many DAPI positive cells that did not pick up the immunostains (e.g. see yellow arrow in figure 5d) were easily identified, demonstrating specificity.

Confirmation of enhanced ROS signaling by chemiluminescence assays

20-5,14-HEDGE treatment increased chemiluminescence in lung tissues greater than that evoked by vehicle (figure 6), consistent with increased superoxide production by this lipid. The rate of change in relative light units per gm tissue per minute was greater in 20-5,14-HEDGE than vehicle treated samples (195 ± 25 for 20-HETE compared to 87 ± 14 for vehicle; p=0.029 Rank Sum test).

Protection from Apoptosis/TUNEL staining by 20-5,14-HEDE in lung slices

We next assessed a second physiological endpoint with intact thick lung tissue sections, protection by 20-HETE against apoptosis, after exposure to hypoxia and reoxygenation

(HR). HR increased apoptosis detected by fluorescent TUNEL in lung slices (figure 7). Treatment with 20-5,14-HEDE protected lung cells from apoptosis.

Confirmation of apoptosis by caspase 3 assays

We confirmed the effect of HR on apoptosis of lung tissue by measuring caspase-3 activity, a common biochemical index of apoptosis. HR increased caspase-3 over that of normoxic control (figure 8), and 20-5,14-HEDE treatment blunted HR-induced increases in caspase-3 activity from homogenates of *ex vivo* lung slices. These data confirm the apoptosis/necrosis of lung cells as determined by TUNEL using caspase 3 activity assays.

Discussion

We have identified increased ROS signaling from ECs within intact lung tissue treated with 20-5,14-HEDGE or 20-5,14-HEDE *ex vivo* in a manner which is qualitatively similar to that of cultured PAECs exposed to the same analogs. These particular analogs were selected for study because 20-5,14-HEDGE protects lungs injured by ischemia reperfusion [10] and 20-5,14-HEDE decreases apoptosis in pulmonary arteries and ECs stressed by HR or lipopolysaccharide [4] in an ROS-dependent manner. Detection of superoxide by DHE fluorescence is not affected by paraformaldehyde fixation, which permits identification of cell-specific signals by immunostaining. 20-5,14-HEDGE-stimulated ROS in this model is confirmed by blocking with PEG-SOD and by chemiluminescence assays. In a second model of injury that is related to ROS, 20-5,14-HEDE protected pulmonary cells in *ex vivo* lung from hypoxia followed by reoxygenation. These data demonstrate that 20-HETE- or analog-stimulated production of ROS which we have reported in cultured ECs [3,4] occurs when ECs are juxtaposed with surrounding vascular smooth muscle and other pulmonary cells *in situ*. Importantly, they define a model which permits investigation of cell-specific ROS and apoptosis signaling pathways evoked by 20-HETE analogs or other bioactivators in intact lung tissue.

ROS, including superoxide and hydrogen peroxide, signal growth, activation of transcription factors, and activation of protein kinases, including ERK, p38 MAPK, and Akt in a variety of cells and injury models [12]. 20-HETE stimulates superoxide, hydrogen peroxide, and nitric oxide production in cultured BPAECs [3,5,13]. 20-HETE- or analog-induced phosphorylation of eNOS enhances NO production via PI3 kinase/Akt, NADPH oxidase and hydrogen peroxide dependent pathways [3]. 20-HETE associated protection against starvation-induced apoptosis in BPAECs or hypoxia reoxygenation injury in *ex vivo* pulmonary arteries depends on stimulated ROS production, as well as NADPH oxidase and PI3K/Akt activation [4]. Together, the studies tie increased ROS production to enhanced survival in cultured pulmonary artery endothelial cells or *ex vivo* PAs. These signaling pathways are well consistent with reports of transcriptional activation of eNOS via Ca21/calmodulin-dependent protein kinase II and hydrogen peroxide in cultured bovine aortic endothelial cells [14,15]. The present work extends observations of 20-HETE or analog evoked-stimulation of ROS and protection from HR injury to *ex vivo* lung tissue. The data in this report do not causally link these actions in intact lung. They also do not address the capacity of native 20-HETE, either endogenously formed or exogenously supplied, to increment ROS or protect from HR injury in intact lung. But the ROS-dependent protective effects of 20-5,14-HEDE in PAECs and *ex vivo* PAs and salutary actions of 20-5,14-HEDGE in ischemic reperfused lung make the hypothesis of cause and effect attractive for future investigations.

Lung slices have been used for more than 60 years for *in vitro* physiologic investigations [16]. More recently investigators have pioneered measurements of ion channel activity [17], and endothelial-dependent modulation of airway and pulmonary vasculature [18] in lung

slices. Similarly, confocal imaging with fluorescent markers has been employed to identify specific anatomical targets such as neuroepithelial bodies in live lung slices [6] or calcium transients in airway smooth muscle cells [7]. Most recent confocal imaging investigations of lungs have employed agarose filled airways [6,7]. We attempted confocal imaging agarose filled lungs labeled with DHE, but the quality of the signal in these cases was degraded and diffuse. Kotlikoff and Tallini [19] noted the extraordinary value of *ex vivo* preparations in which physiological relationships between structures in the lung were preserved “in all their complexity”. Our work advances this goal one step further.

Luminol-enhanced chemiluminescence in rat mesenteric tissue [11] or lung [20] affords a relatively inexpensive and simple estimate of ROS generation. We used chemiluminescence (figure 6) to confirm 20-5,14-HEDE induced increases in ROS production in whole lung (figure 3b), data which extend our previous observations of increased DHE production in cultured pulmonary artery endothelial cells by 20-HETE or 20-5,14-HEDE [4,5]. To determine the contribution of ECs to the stimulated increase in ROS, we loaded lung slices with DHE, then labeled ECs with a primary antibody to PECAM-1, and quantified signal in dual labeled cells. In published data from other investigators relevant to our studies, DHE fluorescence in lung slices following pulmonary artery ligation *in vivo* is increased, and representative images show colocalization of DHE with the endothelial cell marker CD31 [21]. However in that study, quantitative comparison of DHE fluorescence intensity localized to endothelial cells in 3-dimensions from lungs with ligated PAs and control lungs was not performed. DHE signals from isolated pressurized pulmonary arteries are increased in rats exposed to chronic hypoxia [22], but the contribution of specific cell types to this signal was not investigated. Similarly, ROS production (detected by DCF or DHE) by subpleural pulmonary microvascular ECs identified by acetylated LDL uptake has been described [23]. However, even in this elegant model of *in situ* ROS production, signals from non-ECs or ECs from large and small vessels simultaneously could not be detected.

Detection of apoptosis by TUNEL staining is well accepted in most tissues including lungs doubled labeled with an antibody for determination of cell type in lung sections (e.g. reference [24]). Our own work demonstrated protection of pulmonary artery ECs in culture from apoptosis by 20-5,14-HEDE [4]. The present studies show 20-5,14-HEDE protection of pulmonary tissue *in situ* from HR injury. Of interest is the observation by Umachandran *et al* [25] who reported metabolic activity of 600 micron thick cultured lung slices towards 7-ethoxycoumarin for 8 hours. Though our studies did not evaluate metabolic activity, we demonstrate very limited TUNEL staining in cultured lung slices maintained in normoxia, but impressive increases in samples from hypoxia for 6 hours followed by reoxygenation.

Conclusions

We report modulation of ROS signaling and apoptosis by 20-HETE analogs in sections of lung having intact cell-cell and cell-matrix interactions. Our results identify ROS production and protective effects of these fatty acids in lung tissue, extending our previous reports of superoxide induced protection of cultured pulmonary artery endothelial cells by 20-HETE. This model may also provide the ability to test multiple interventions from the same preparation under well-controlled conditions, and identifies signals from discrete cell types simultaneously.

Acknowledgments

The authors acknowledge contributions of Stephanie Gruenloh, Ying Gao and Brian Weinberg and other members of the Jacobs and Medhora labs. Confocal microscopy was facilitated by Drs. Paula North, Suresh Kumar, and the Children’s Research Institute Imaging Core Laboratory. Financial support was provided by the Robert A. Welch

Foundation (GL 625910) and NIH (DK38226; JRF)(HL49294; ERJ). This material is the result of work supported with resources and the use of facilities at the Clement J. Zablocki VA Medical Center.

Abbreviations

20-HETE	20-hydroxyeicosatetraenoic acid
BPAEC	Bovine pulmonary artery endothelial cell
DCF	Dichlorofluorescein
DHE	Dihydroethidium
DMEM	Dulbecco's modified essential media
EC	Endothelial cell
FITC	Fluorescein isothiocyanate
LDL	Low Density Lipoprotein
PECAM	Platelet endothelial cell adhesion molecule
PEG-SOD	Polyethylene glycol coupled superoxide dismutase
PBS	Phosphate buffered saline
HR	Hypoxia-reoxygenation
ROI	Region of interest
ROS	Reactive oxygen species
TUNEL	Terminal deoxynucleotidyl transferase mediated dUTP Nick End Labeling

Bibliography

1. Harder DR, Roman RJ. Endothelial dysfunction and hypertension in rats transduced with CYP4A2 adenovirus. Circ Res. 2006; 98:866–867. [PubMed: 16614311]
2. Harder DR, Narayanan J, Gebremedhin D. Pressure-induced myogenic tone and role of 20-HETE in mediating autoregulation of cerebral blood flow. Am J Physiol Heart Circ Physiol. 2011; 300:H1557–65. [PubMed: 21257913]
3. Bodiga S, Gruenloh SK, Gao Y, Manthati VL, Dubasi N, Falck JR, Medhora M, Jacobs ER. 20-HETE-induced nitric oxide production in pulmonary artery endothelial cells is mediated by NADPH oxidase, H2O2, and PI3-kinase/Akt. Am J Physiol Lung Cell Mol Physiol. 2010; 298:L564–74. [PubMed: 20061439]
4. Dhanasekaran A, Bodiga S, Gruenloh S, Gao Y, Dunn L, Falck JR, Buonaccorsi JN, Medhora M, Jacobs ER. 20-HETE increases survival and decreases apoptosis in pulmonary arteries and pulmonary artery endothelial cells. Am J Physiol Heart Circ Physiol. 2009; 296:H777–86. [PubMed: 19136601]
5. Medhora M, Chen Y, Gruenloh S, Harland D, Bodiga S, Zielonka J, Gebremedhin D, Gao Y, Falck JR, Anjaiah S, Jacobs ER. 20-HETE increases superoxide production and activates NAPDH oxidase in pulmonary artery endothelial cells. Am J Physiol Lung Cell Mol Physiol. 2008; 294:L902–11. [PubMed: 18296498]
6. Bergner A, Sanderson MJ. Airway contractility and smooth muscle Ca(2+) signaling in lung slices from different mouse strains. J Appl Physiol. 2003; 95:1325–32. discussion 1314. [PubMed: 12777405]
7. Pintelon I, De Proost I, Brouns I, Van Herck H, Van Genechten J, Van Meir F, Timmermans JP, Adriaensen D. Selective visualisation of neuroepithelial bodies in vibratome slices of living lung by 4-di-2-ASP in various animal species. Cell Tissue Res. 2005; 321:21–33. [PubMed: 15902500]
8. Popov TA. Human exhaled breath analysis. Ann Allergy Asthma Immunol. 2011; 106:451–6. quiz 457. [PubMed: 21624743]

9. Jacobs ER, Effros RM, Falck JR, Reddy KM, Campbell WB, Zhu D. Airway synthesis of 20-hydroxyeicosatetraenoic acid: Metabolism by cyclooxygenase to a bronchodilator. Am J Physiol. 1999; 276:L280–8. [PubMed: 9950890]
10. Ali I, Gruenloh S, Gao Y, Clough A, Falck JR, Medhora M, Jacobs ER. Protection by 20-5,14-HEDGE against surgically induced ischemia reperfusion lung injury in rats. Ann Thorac Surg. 2012; 93:282–288. [PubMed: 22115333]
11. Whitehouse JS, Xu H, Shi Y, Noll L, Kaul S, Jones DW, Pritchard KA Jr, Oldham KT, Gourlay DM. Mesenteric nitric oxide and superoxide production in experimental necrotizing enterocolitis. J Surg Res. 2010; 161:1–8. [PubMed: 19922948]
12. Gutterman DD. Mitochondria and reactive oxygen species: An evolution in function. Circ Res. 2005; 97:302–304. [PubMed: 16109924]
13. Chen Y, Medhora M, Falck JR, Pritchard KA Jr, Jacobs ER. Mechanisms of activation of eNOS by 20-HETE and VEGF in bovine pulmonary artery endothelial cells. Am J Physiol Lung Cell Mol Physiol. 2006; 291:L378–85. [PubMed: 16679377]
14. Cai H, Davis ME, Drummond GR, Harrison DG. Induction of endothelial NO synthase by hydrogen peroxide via a ca(2+)/calmodulin-dependent protein kinase II/janus kinase 2-dependent pathway. Arterioscler Thromb Vasc Biol. 2001; 21:1571–1576. [PubMed: 11597928]
15. Drummond GR, Cai H, Davis ME, Ramasamy S, Harrison DG. Transcriptional and posttranscriptional regulation of endothelial nitric oxide synthase expression by hydrogen peroxide. Circ Res. 2000; 86:347–354. [PubMed: 10679488]
16. Barron ES, Miller ZB, Bartlett GR. Studies on biological oxidations; the metabolism of lung as determined by a study of slices and ground tissue. J Biol Chem. 1947; 171:791–800. [PubMed: 20272118]
17. Bourke S, Mason HS, Borok Z, Kim KJ, Crandall ED, Kemp PJ. Development of a lung slice preparation for recording ion channel activity in alveolar epithelial type I cells. Respir Res. 2005; 6:40. [PubMed: 15857506]
18. Moreno L, Perez-Vizcaino F, Harrington L, Faro R, Sturton G, Barnes PJ, Mitchell JA. Pharmacology of airways and vessels in lung slices in situ: Role of endogenous dilator hormones. Respir Res. 2006; 7:111. [PubMed: 16923180]
19. Kotlikoff MI, Tallini NY. Imaging dynamic cellular events in the lung. J Gen Physiol. 2005; 125:529–530. [PubMed: 15928399]
20. Hemnes AR, Zaiman A, Champion HC. PDE5A inhibition attenuates bleomycin-induced pulmonary fibrosis and pulmonary hypertension through inhibition of ROS generation and RhoA/Rho kinase activation. Am J Physiol Lung Cell Mol Physiol. 2008; 294:L24–33. [PubMed: 17965319]
21. Nijmeh J, Moldobaeva A, Wagner EM. Role of ROS in ischemia-induced lung angiogenesis. Am J Physiol Lung Cell Mol Physiol. 2010; 299:L535–41. [PubMed: 20693319]
22. Broughton BR, Jernigan NL, Norton CE, Walker BR, Resta TC. Chronic hypoxia augments depolarization-induced Ca2+ sensitization in pulmonary vascular smooth muscle through superoxide-dependent stimulation of RhoA. Am J Physiol Lung Cell Mol Physiol. 2010; 298:L232–42. [PubMed: 19897743]
23. Zhang Q, Chatterjee S, Wei Z, Liu WD, Fisher AB. Rac and PI3 kinase mediate endothelial cell-reactive oxygen species generation during normoxic lung ischemia. Antioxid Redox Signal. 2008; 10:679–689. [PubMed: 18162054]
24. Qiu H, Orr FW, Jensen D, Wang HH, McIntosh AR, Hasinoff BB, Nance DM, Pylypas S, Qi K, Song C, Muschel RJ, Al-Mehdi AB. Arrest of B16 melanoma cells in the mouse pulmonary microcirculation induces endothelial nitric oxide synthase-dependent nitric oxide release that is cytotoxic to the tumor cells. Am J Pathol. 2003; 162:403–412. [PubMed: 12547699]
25. Umachandran M, Howarth J, Ioannides C. Metabolic and structural viability of precision-cut rat lung slices in culture. Xenobiotica. 2004; 34:771–780. [PubMed: 15690764]

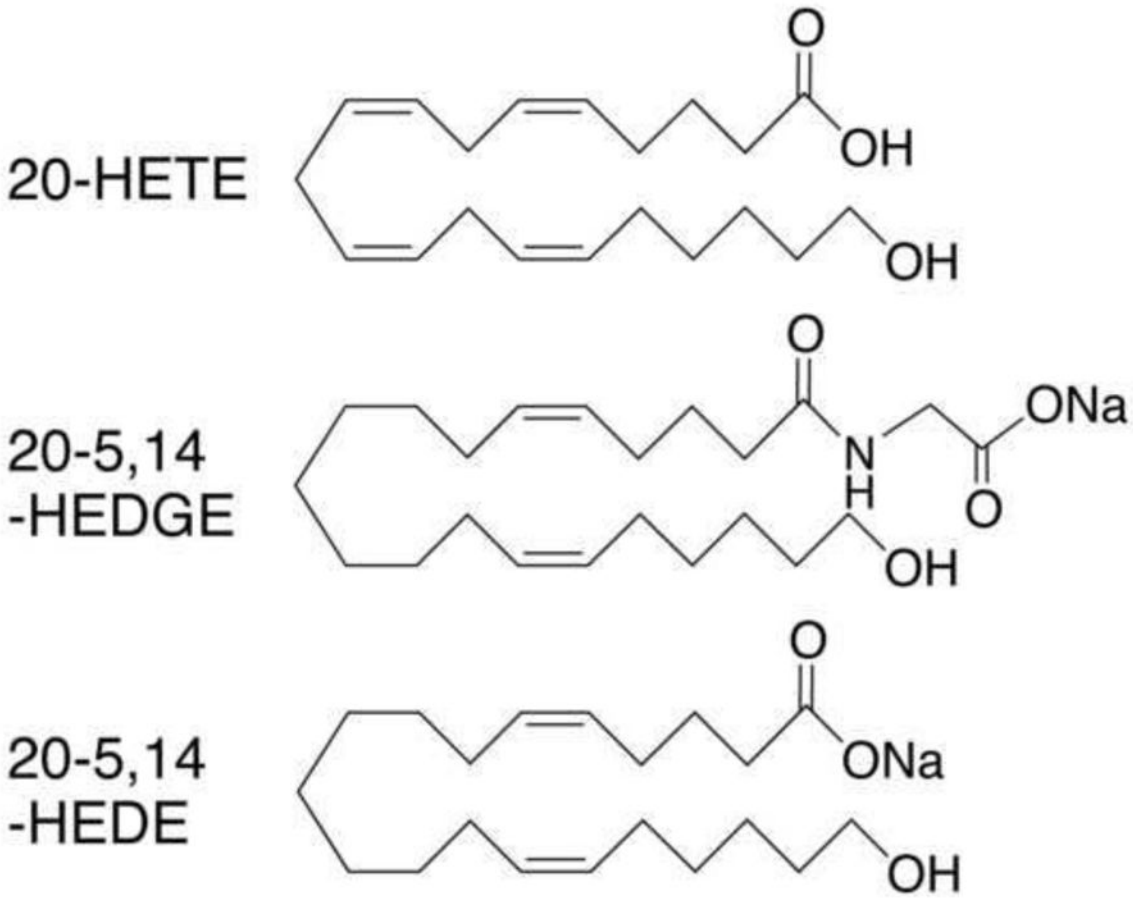

Figure 1.
Chemical structure of 20-HETE, 20-5,14-HEDE and 20-5,14-HEDGE.

Figure 2a

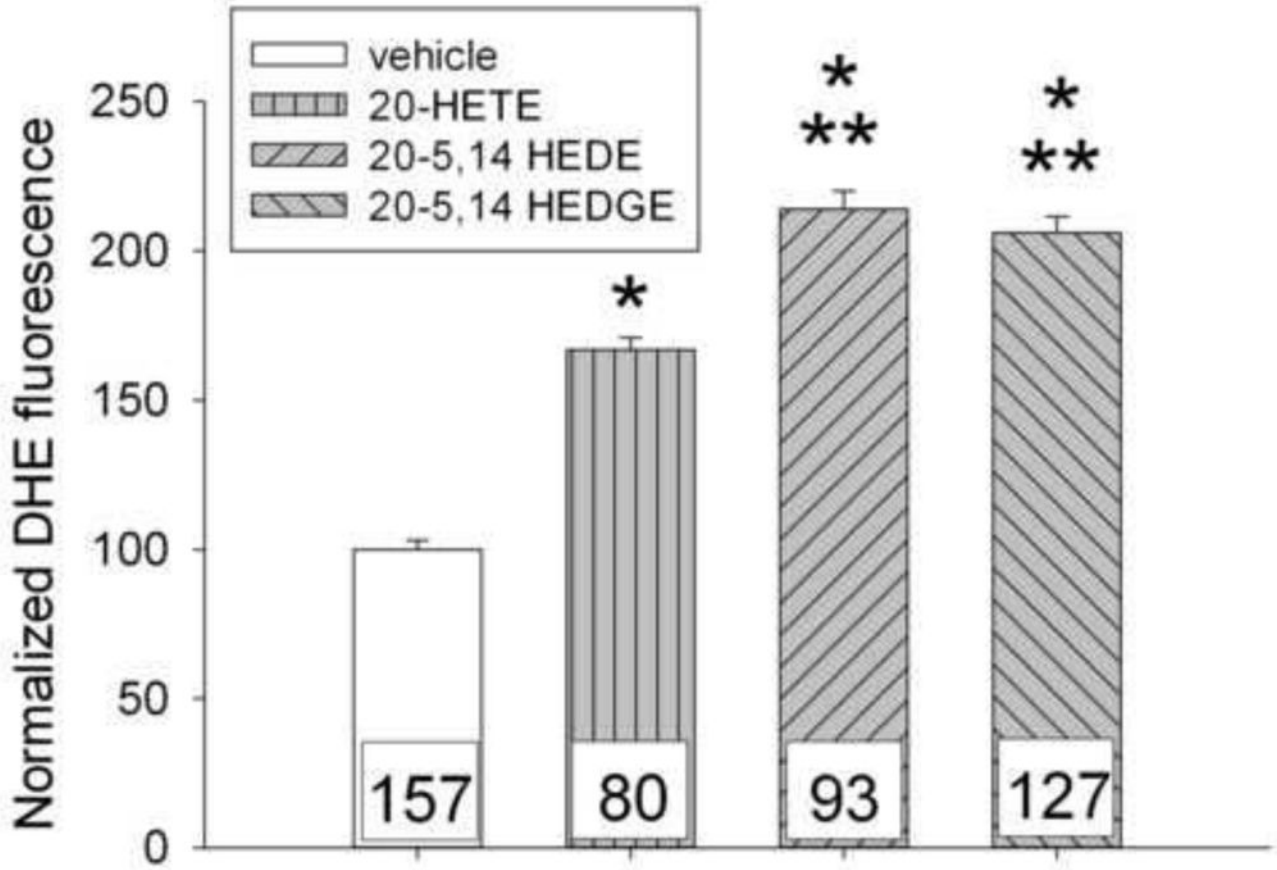

Figure 2b

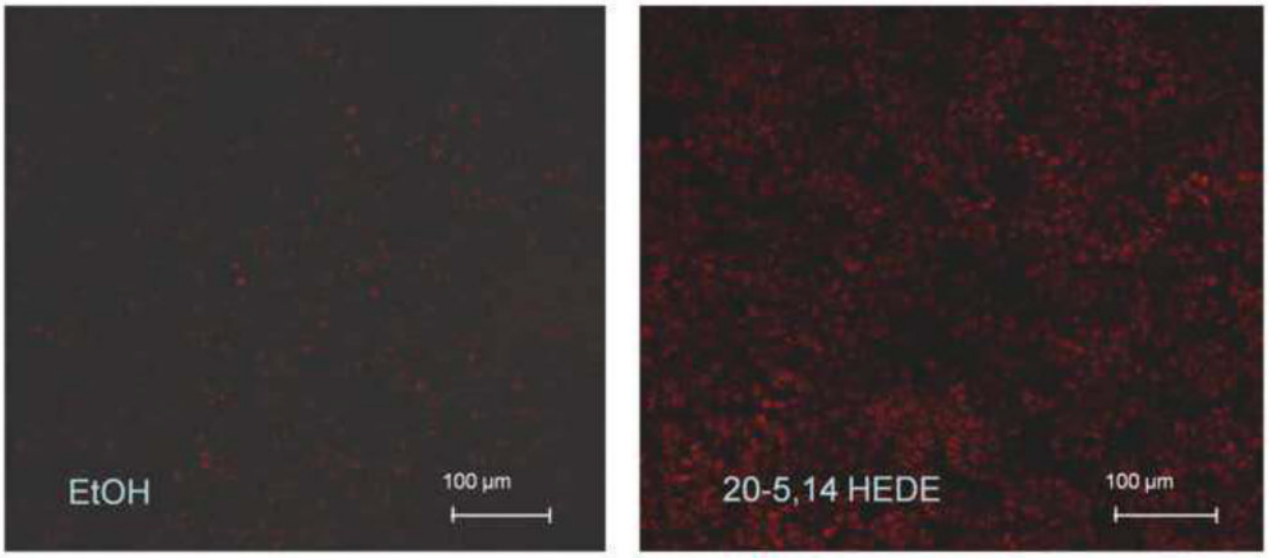

Figure 2c

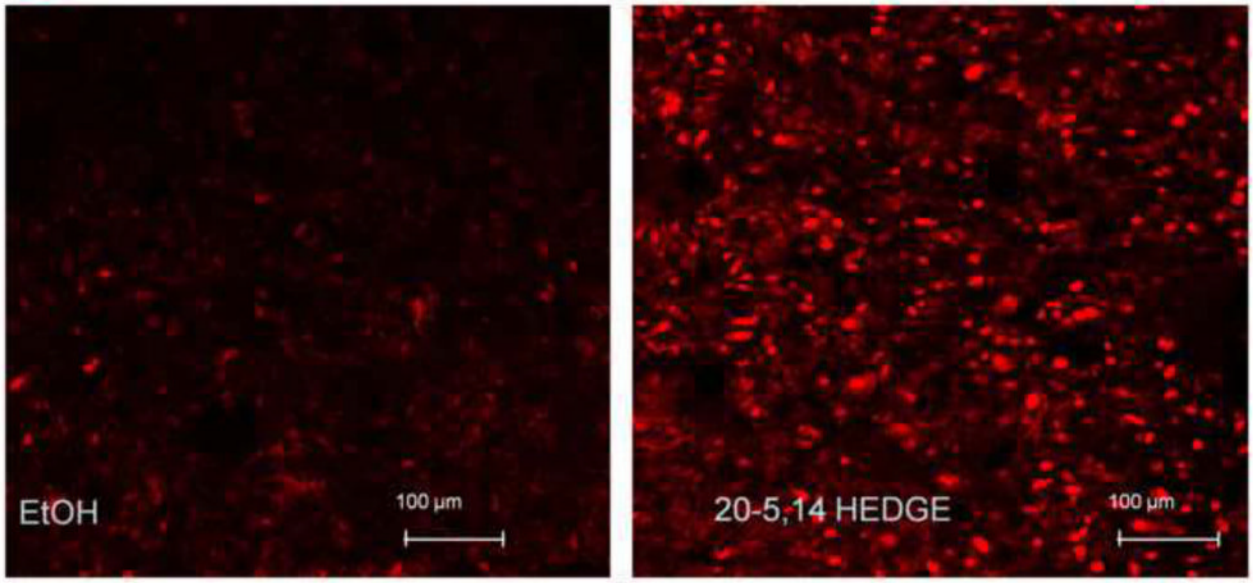

Figure 2d

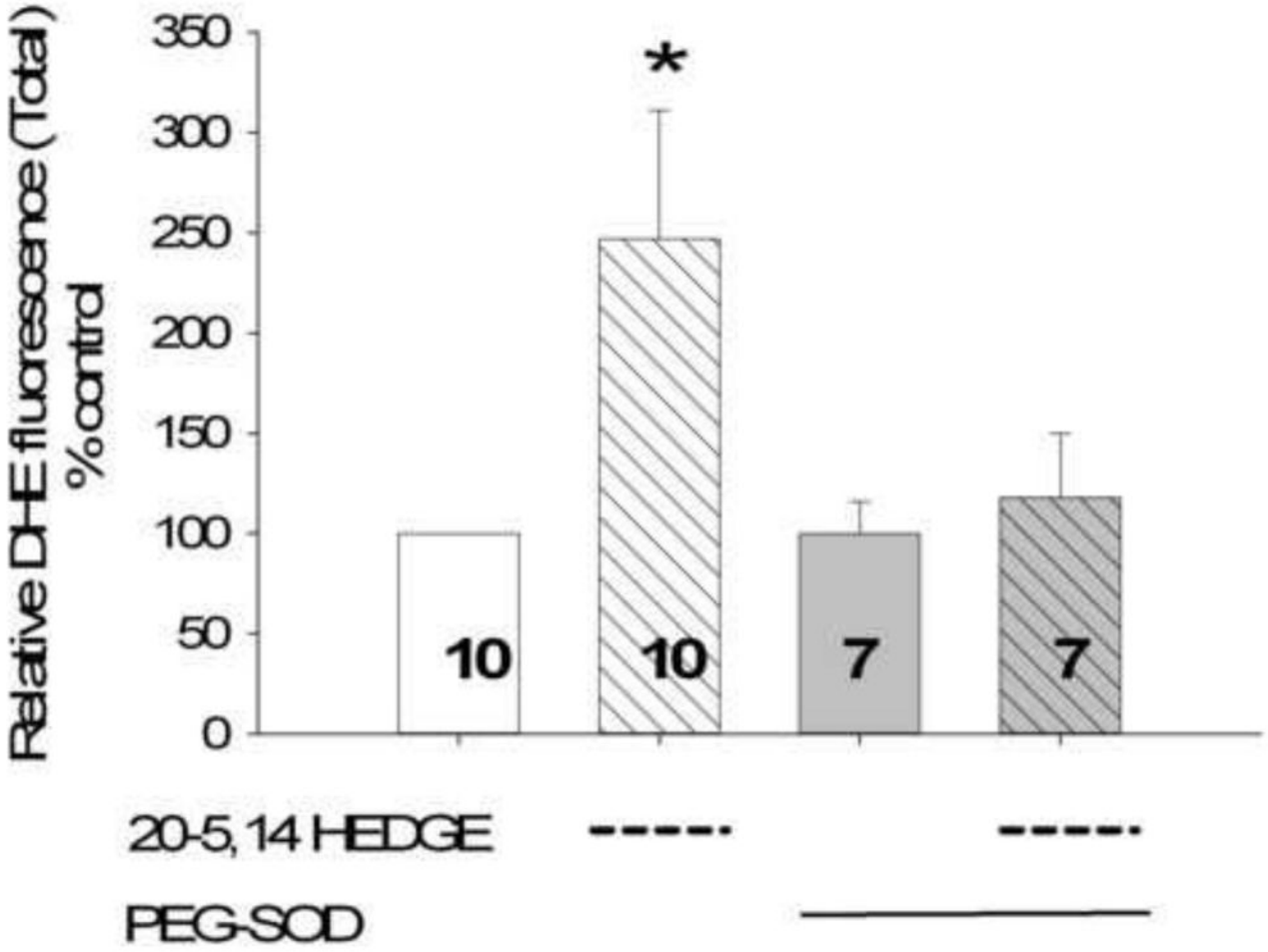

Figure 2.

Figure 2a. DHE fluorescence intensity in cultured bovine pulmonary artery endothelial cells ~10 minutes after addition of ethanol vehicle, 1 μM 20-HETE, 1 μM 20-5,14-HEDE or 1 μM 20-5,14-HEDGE. Data are normalized to the average fluorescence intensity of cells treated with vehicle in order to permit comparisons across several groups of cells. The numbers within the bars represent the number of cells analyzed in each group. "*" indicates $p<0.01$ relative to vehicle control. "**" indicates $p<0.001$ relative to vehicle control and 20-HETE.

Figure 2(b) and 2(c). Representative confocal images from unfixed lung slices stained with DHE, then exposed for 15 minutes to 1 μM 20,5-14 HEDE, 1 μM 20,5-14 HEDGE or ethanol (vehicle). In these images, the lacy pattern of fixed inflated lungs is less apparent due to lack of inflation, but an increase in DHE fluorescence in samples treated with either analog - as opposed to vehicle-treated samples is evident. (d) mean ± SEM fluorescence values of lung sections treated with vehicle or 20,5-14 HEDGE with or without 100 IU PEG SOD. Values are normalized to those of vehicle control. Pilot studies of lung sections treated with 250 IU PEG SOD did not exhibit further decrease in fluorescence above that of samples treated with 100 IU PEG-SOD. Averaged data for samples treated with 100 IU

PEG-SOD are shown. “*” indicates that the DHE signal was brighter in 20,5-14 HEDGE -treated than vehicle- or PEG-SOD-treated samples ($p<0.05$).

Figure 3a

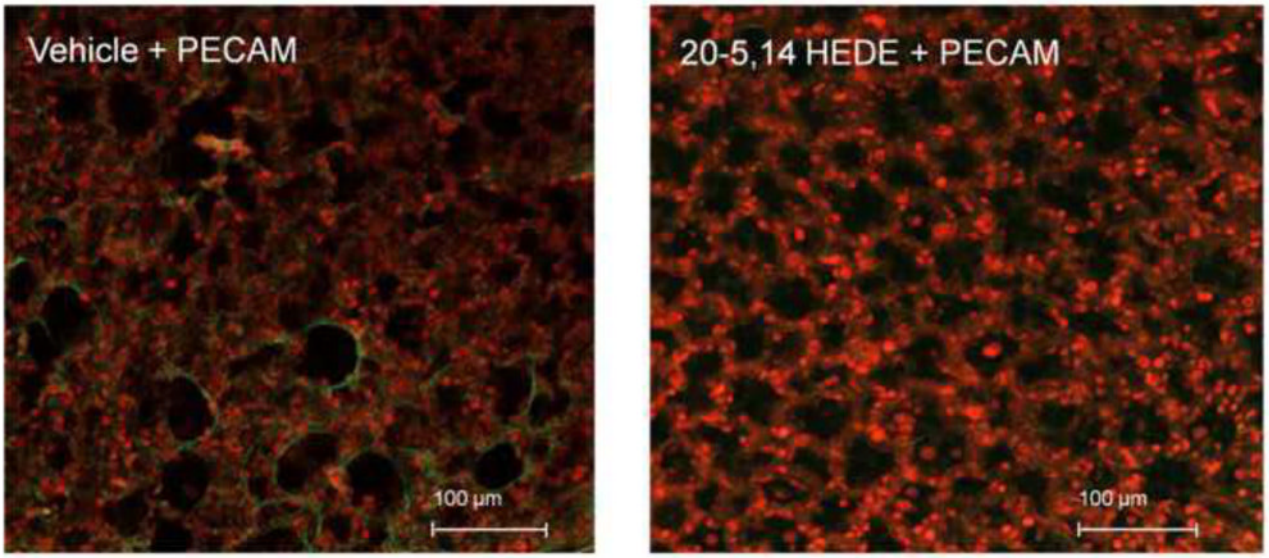

Figure 3b

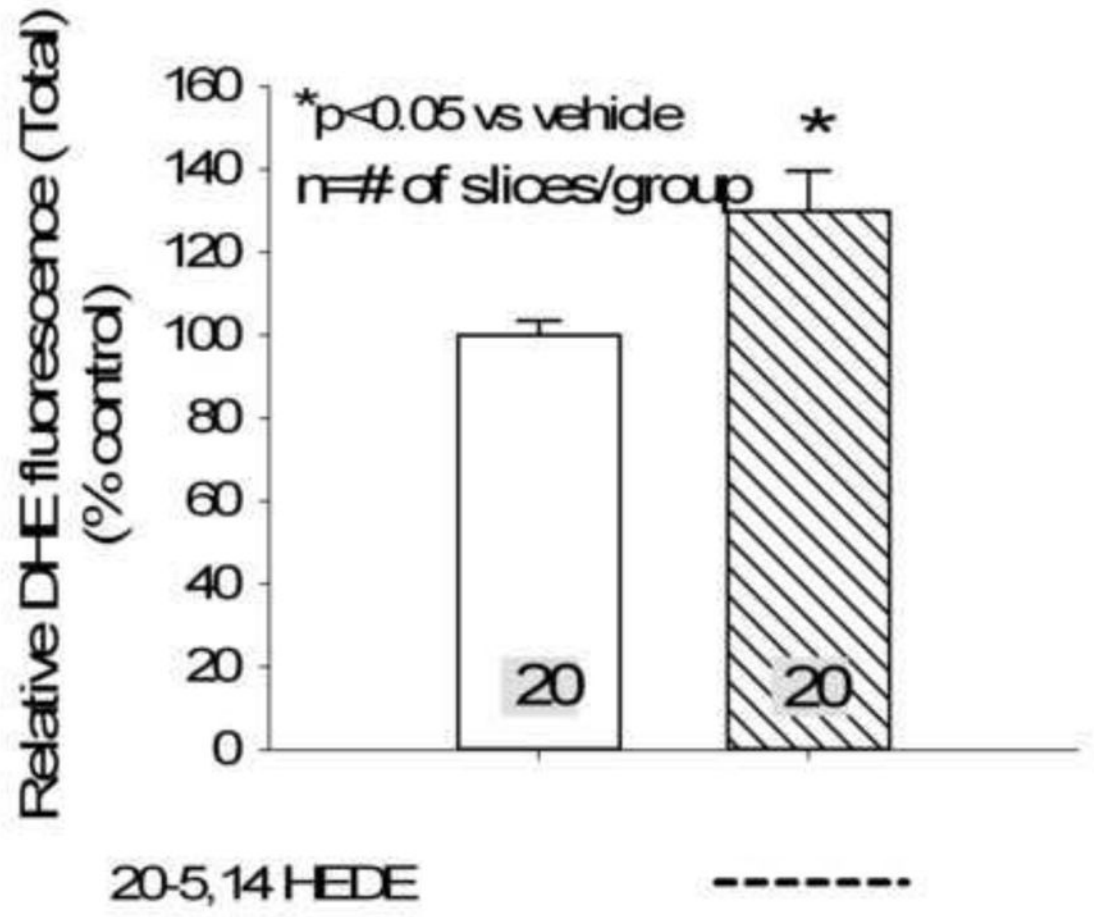

Figure 3.

(a) Confocal images of lung sections loaded with DHE, treated with 20-5,14-HEDE or vehicle, fixed with paraformaldehyde then probed with antibody to PECAM-1 are shown. The images show increased DHE fluorescence in sections treated with 20-5,14-HEDE versus vehicle control. (b) Averaged DHE fluorescence intensity from 20 confocal slices of vehicle-treated and 20 slices of 20-5,14-HEDE treated sections. These data were obtained from 4 separate experiments with 5 slices from each obtained around the peak of fluorescence.

Figure 4a

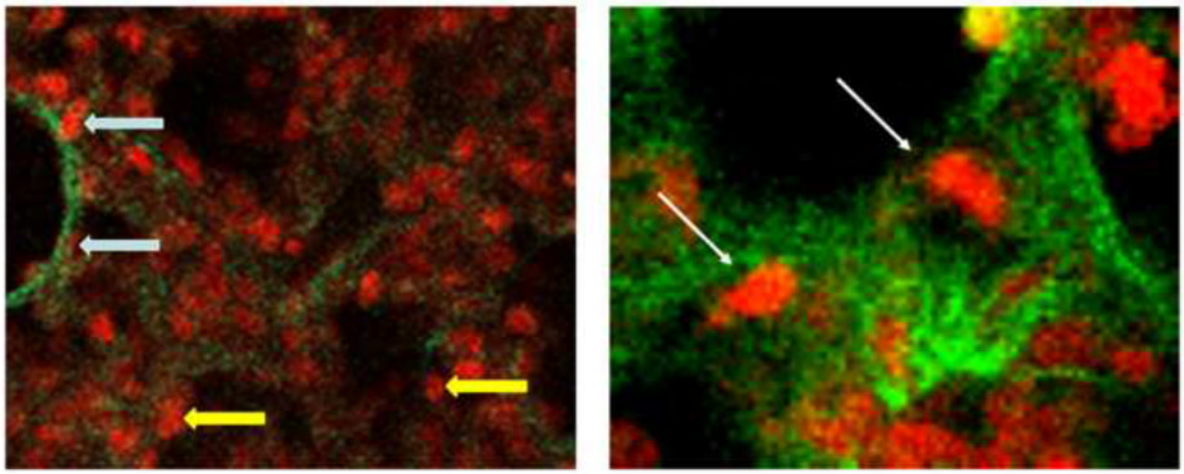

Figure 4b

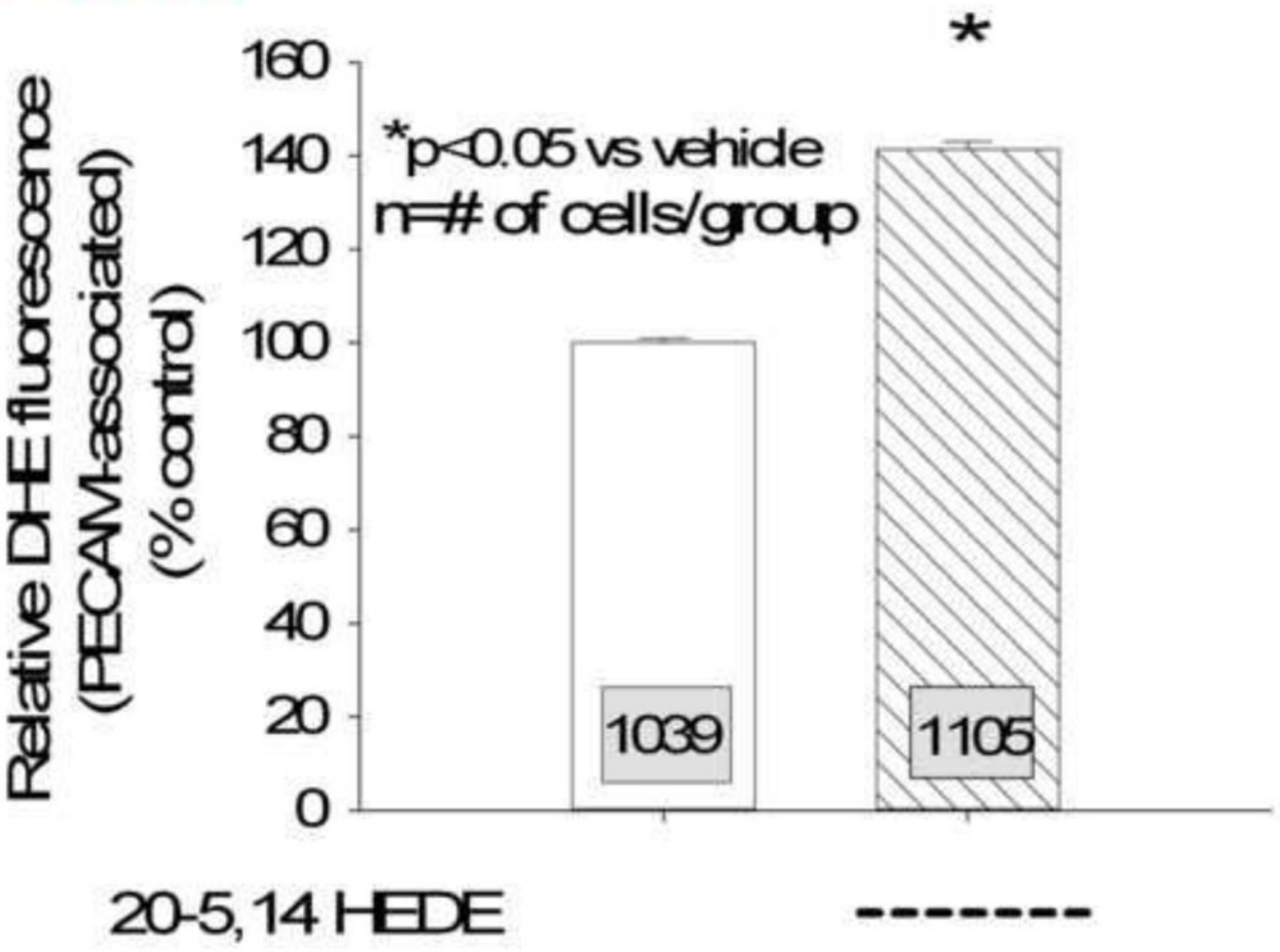

Figure 4.

(a) Two representative confocal images at high power from lungs loaded with DHE, treated with 20-5,14-HEDE or vehicle, fixed, and then probed with a primary antibody to PECAM-1. The white arrows identify PECAM associated cells, whereas the two yellow arrows show DHE fluorescence in cells that do not appear to be associated with PECAM-1. (b) DHE fluorescence in more than 1000 ROIs each identified as PECAM-1 associated, in confocal images from lung slices treated with either vehicle or 20-5,14-HEDE. Data are normalized to mean fluorescence in vehicle-treated samples (since paired samples from 4 separate rats were obtained in different settings). 20-5,14-HEDE increased ROS in pulmonary artery ECs as compared to vehicle (ethanol) treatments.

Figure 5a

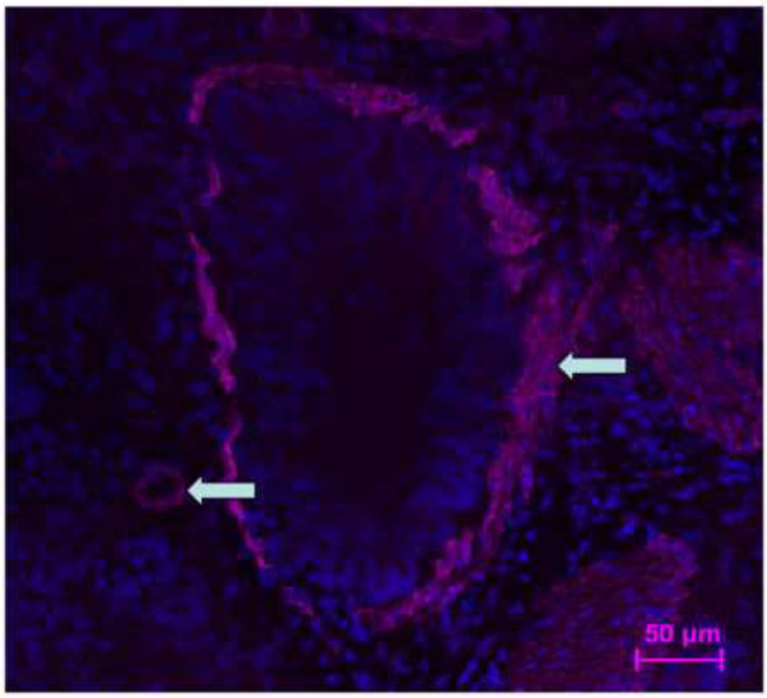

Figure 5b

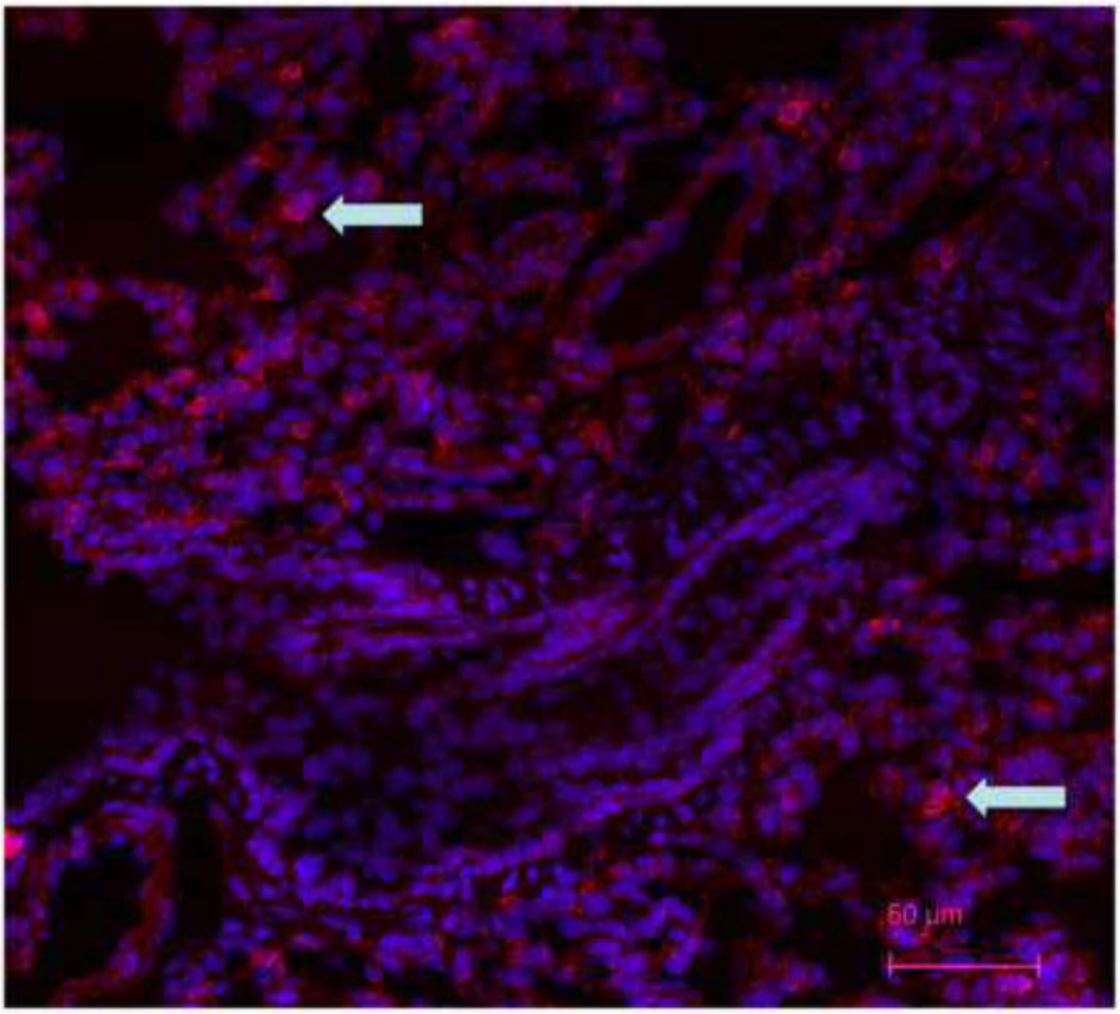

Figure 5c

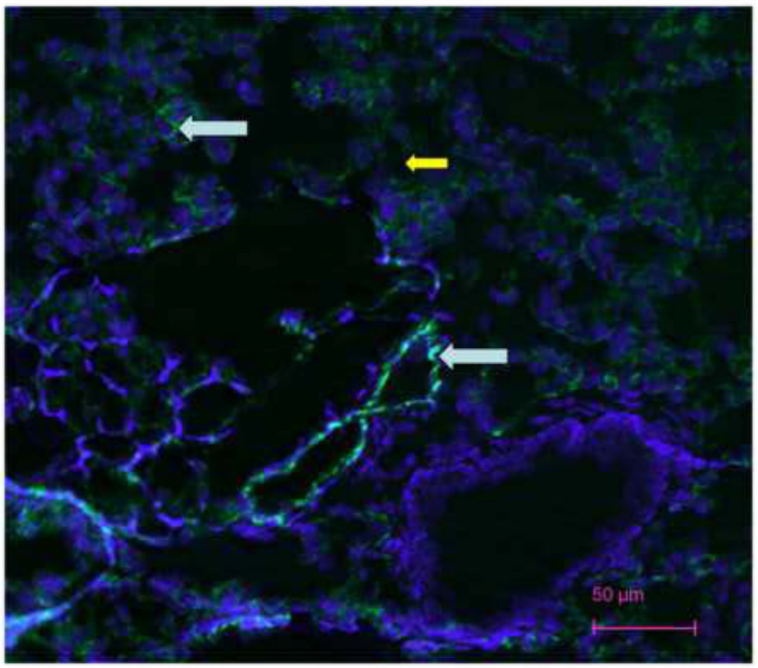

Figure 5d

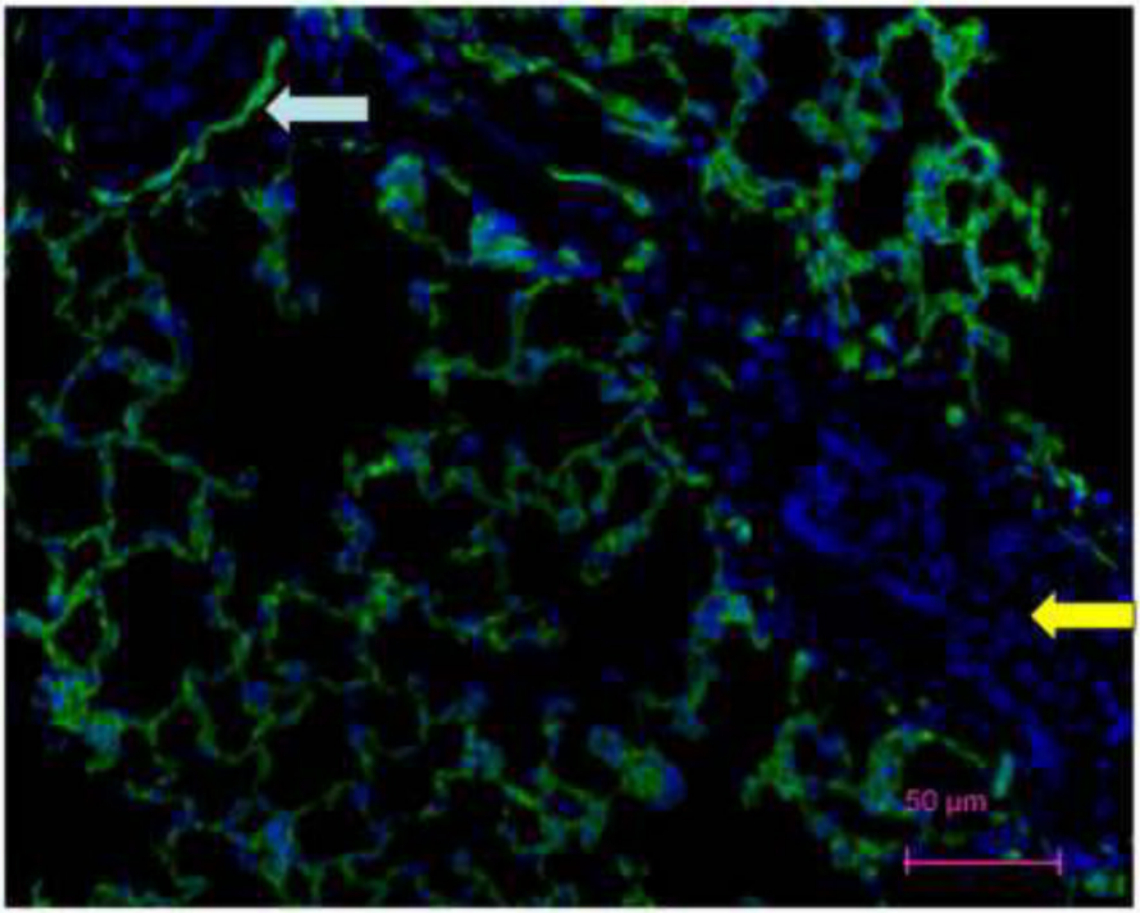

Figure 5.

Thin sections of OTC embedded, acetone-fixed lung immunostained with primary antibody to smooth muscle actin (5a), alpha keratin (5b) or CD31 (5c) and counterstained with DAPI. (a) Immunostaining is identified as dark pink in a pan-cytoplasmic distribution within smooth muscle cells around airways and blood vessels (arrows), consistent with high expression of this cytoskeletal protein in these cells. (b) Immunofluorescence for cytoskeleton component cytokeratin 7 is identified primarily in junctions between epithelial cells. (c) CD31 green fluorescence in the distribution of plasma membranes of endothelial cells (arrows identify small blood vessel and capillary endothelial cells). In each section, DAPI identifies the nuclei of cells, many of which are negative for the immunostain. The white arrows pointing to green PECAM-1 positive staining. The yellow arrow points to non-immunostained DAPI positive cells. (d) Because our confocal studies with immunostaining were performed on sections fixed with paraformaldehyde, and our images in figure1a-c were obtained from acetone fixed tissue, we performed an additional set of studies. 300 micron thick sections of tissue were fixed in paraformaldehyde, then immunostained with CD31 and counterstained with DAPI. Frozen sections of these tissues 4 microns thick were imaged with a Nikon Eclipse TE2000-U with a camera attachment (Qimaging QCAM FAST394) for epifluorescence. In these images, a pattern of plasma membrane uptake is evident in

some (marked with white arrow) but not all (marker with yellow arrow) cells, similar to that in acetone fixed and OTC treated sections.

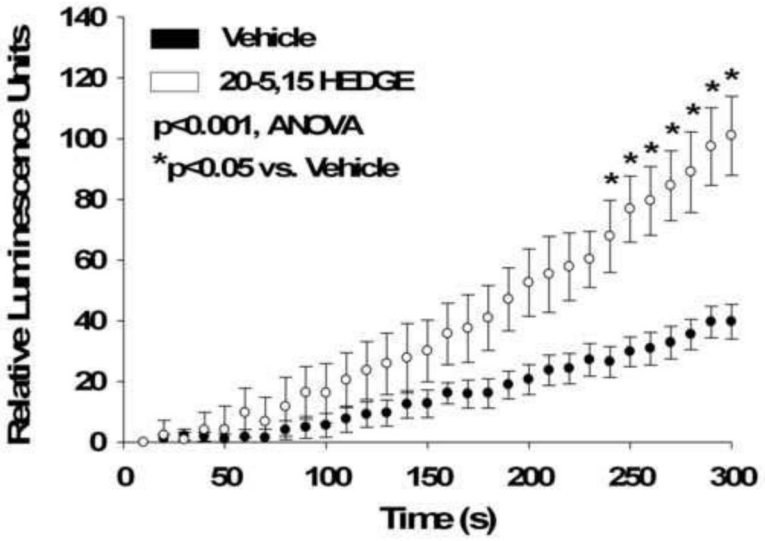

Figure 6.

Chemiluminescence of lung samples treated with 20-5,14-HEDGE or vehicle. Average weights of lung tissues were 19.5 ± 1 mg (vehicle) and 19.9 ± 1 mg (20-5,14-HEDGE; p=0.74, n.s.). Lung pieces were incubated with 20-5,14-HEDGE or vehicle for 15 minutes followed by addition of lucigenin. Luminescence was then detected every 10s for 5 minutes. “n” =4 samples for vehicle and 7 samples for 20-5,14-HEDGE. Bars represent standard error of the means. 20-5,14-HEDGE increased chemiluminescence over time above that of vehicle treated samples. “*” indicates increased over vehicle treated control samples at the same time period after addition of 20-5,14-HEDGE ($p<0.05$).

Figure 7a

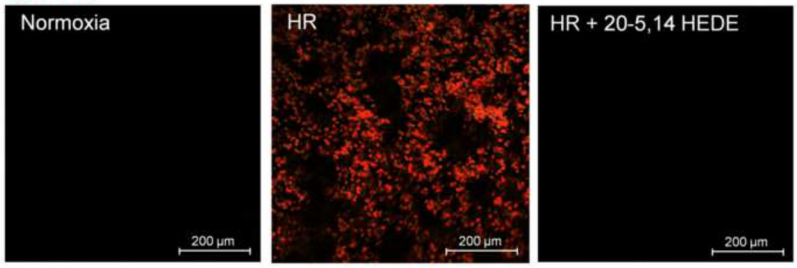

Figure 7b

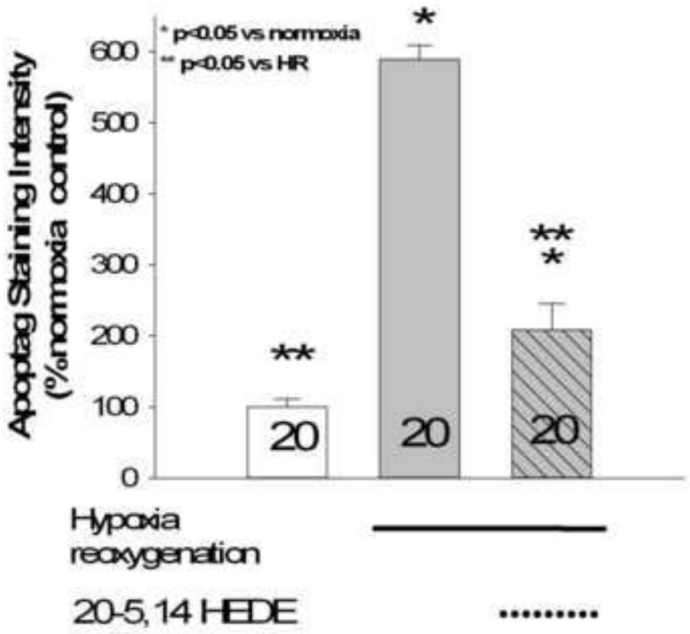

Figure 7.

(a) Representative images of lung slices treated with (1) normoxia and vehicle control (2) hypoxia followed by reoxygenation (HR) with vehicle treatment or (3) HR with treatment by 20-5,14-HEDE immediately before hypoxia. At the end of reoxygenation, slices were fixed and probed for TUNEL positive cells (appears as red). HR increased the number of TUNEL-positive cells. Treatment with 20-5,14-HEDE blocked this increase. (b) Average fluorescence intensity of TUNEL staining in 3 treatment groups. HR increased the intensity of TUNEL positivity in lung tissue. 20-5,14-HEDE blunted but did not eliminate HR-evoked increases in TUNEL positivity.

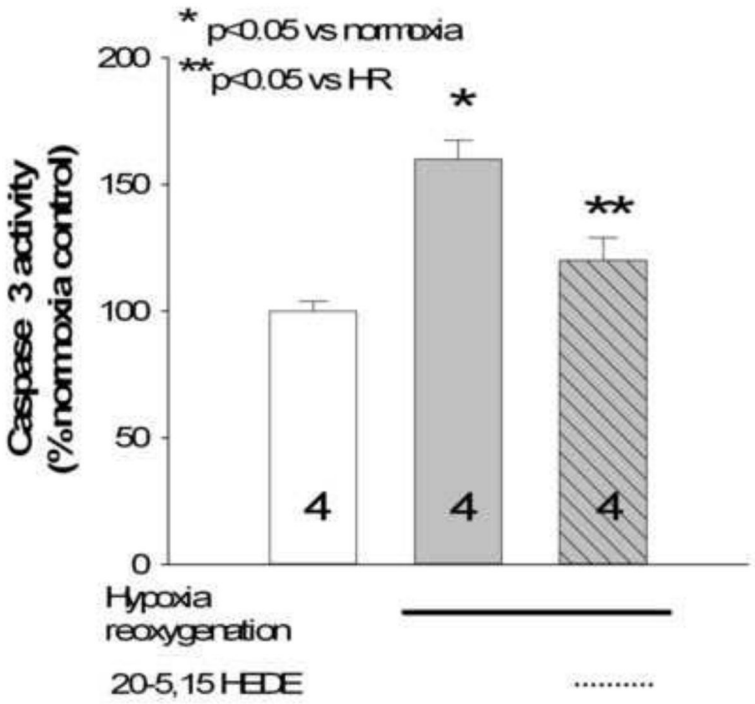

Figure 8.

Caspase-3 activity in homogenates of lung slices treated with normoxia (control), HR, or 20-5,14-HEDE plus HR, conditions identical to those from figure 6. HR increased caspase-3 activity, and this increase was blocked by 20-5,14-HEDE.